

IN-VACUUM UNDULATORS

T. Tanaka*, T. Hara, R. Tsuru, D. Iwaki, X. Marechal, T. Bizen, T. Seike and H. Kitamura
 SPring-8, Koto 1-1-1, Mikazuki, Sayo, Hyogo 679-5148, Japan

Abstract

The so-called in-vacuum undulators, in which magnet arrays are installed inside the vacuum chamber, have been proved to be a promising way toward shorter wavelength of synchrotron radiation (SR). Especially, it has been adopted in lots of medium-scale SR facilities to provide angstrom x rays to carry out protein-crystallography experiments. Needless to say, there have been a number of technical challenges to be overcome for realization of in-vacuum undulators. For example, some measures have to be taken to achieve ultra high vacuum enough to be installed in the storage ring, field correction schemes should be established for utilization of higher harmonics, and so on. Most of these technologies have been established in SPring-8, in which more than 20 in-vacuum undulators have been installed.

INTRODUCTION

One of the most important field in the synchrotron radiation (SR) science is the protein crystallography, which takes advantage of intense x-rays in the angstrom region. For higher brilliance, undulators, but not wigglers, should be used as light sources. It should be noted, however, that only a large-scale SR facility with a high-energy electron beam, such as the ESRF, APS, SPring-8, can provide x-rays with fundamental radiation of conventional undulators having periodic length longer than 50 mm. In order to obtain high-brilliance x rays in the angstrom region, an undulator with periodic length shorter than 20 mm is required. In addition, it should have a good magnetic performance to provide sufficient intensity of higher harmonics. At present, the in-vacuum undulator (IVU) is the only device to meet such a requirement without any problem.

The peak field in the undulator is roughly given by

$$B(G_m) = 1.8\alpha B_r e^{-\pi G_m/\lambda_u},$$

where α is the 3-dimensional geometrical factor of permanent magnet (PM) blocks and is of the order of unity, B_r the remanent field of the PM material, λ_u the undulator period and G_m the magnet gap. In the conventional undulator that has a vacuum chamber between the top and bottom magnet arrays, the magnet gap is always longer than the vacuum gap (G_v), i.e., the inner aperture of the vacuum chamber. The minimum vacuum gap is limited by the storage ring conditions such as the lifetime and injection efficiency. Thus, we have

$$B(G_m) \leq 1.8\alpha B_r e^{-\pi G_v/\lambda_u} e^{-\pi \Delta G/\lambda_u},$$

where ΔG is the difference between the magnet and vacuum gaps determined by the thickness of the vacuum chamber wall and clearance between the vacuum chamber and magnet arrays, being usually around 3 mm.

The concept of the in-vacuum undulator (IVU) is to eliminate ΔG for higher peak field by installing the magnet arrays inside the vacuum chamber. In this case, the vacuum gap is exactly the same as the magnet gap and thus is variable, meaning that a wide clearance is available for the electron beam to pass through the undulator if the magnet gap is fully opened. This also brings a lot of advantages for the accelerator operation.

Although the principle is very simple, a lot of difficulties should be overcome to realize the IVU. For example, ultra high vacuum (UHV) better than, e.g., 10^{-10} Torr, is required to be installed in the storage ring in spite of a large number of components placed in the vacuum chamber. In this paper, key technologies necessary for the IVU are reviewed and several exotic IVUs developed at SPring-8 are introduced. In addition, ongoing R&Ds for future IVU development are described.

HISTORY

The history of IVU development is summarized in Table 1. Because the concept is very simple, a lot of efforts have been devoted to realization of the IVU. The first IVU working regularly was constructed in KEK [1] in 1990 and installed in the TRISTAN Accumulation Ring. It was dedicated to production of hard x-rays ranging from 5 to 25 keV using up to the 5th harmonic. After that, the IVU has been adopted as a standard insertion device (ID) at SPring-8. During the process of mass production, improvements have been made to make it more feasible for operation in the storage ring as a SR source.

A pilot IVU for the SPring-8 was constructed in 1996 [2]. Meanwhile, a lot of know-how necessary for IVU development was accumulated. In 1997, an IVU with the same structure as the pilot one but the total length of 1.5 m was brought to ESRF for a feasibility test using the electron beam [4]. During the test, the SUS sheet that covered the magnet surface to reduce the resistive-wall impedance was fused. Since the temperatures of magnets measured with thermocouples were always constant during the test, and the SUS sheet was non-magnetic, it was concluded that it was fused by deposited heat brought by the resistive-wall heating and SR from the upstream bending magnet. After the test, the Ni-coated Cu sheet has been employed instead of the SUS sheet for better thermal and electrical conductivity.

* ztanaka@spring8.or.jp

Table 1: History of IVU development.

Year	Facility	Contents	Remarks
1990	KEK	$\lambda_u = 40\text{mm}$, $G_{\min} = 10\text{mm}$, $L = 3.6\text{m}$	1st IVU that works regularly
1996	SPring-8	$\lambda_u = 32\text{mm}$, $G_{\min} = 7\text{mm}$, $L = 4.5\text{m}$	1st IVU for SPring-8
1996	SPring-8 & ESRF	$\lambda_u = 24\text{mm}$, $G_{\min} = 5\text{mm}$, $L = 1.5\text{m}$	Beam test of IVU at ESRF
1997	SPring-8	1st on-beam commissioning	4 IVUs have been installed from the beginning
1997~	SPring-8	IVUs with exotic PM configurations	Vertical, helical and figure-8
1997	SPring-8 & NSLS	$\lambda_u = 11\text{mm}$, $G_{\min} = 2\text{mm}$, $L = 0.3\text{m}$	
1999~	SPring-8 & PLS	Demagnetization test of PM material	2GeV linac (PLS), 8GeV synchrotron (SPring-8)
2000	SPring-8	$\lambda_u = 32\text{mm}$, $G_{\min} = 12\text{mm}$, $L = 25\text{m}$	IVU for the long straight section in SPring-8
2000	SPring-8 & SLS	$\lambda_u = 24\text{mm}$, $G_{\min} = 5\text{mm}$, $L = 1.5\text{m}$	Same as that tested at ESRF(magnet refreshed)
2000	SPring-8	$\lambda_u = 6, 15, 20, 24\text{mm}$, $L = 1\text{m}$	Revolver undulator (installed in PLS in 2003)
2001	ESRF	$\lambda_u = 17 \sim 23\text{mm}$, $G_{\min} = 6\text{mm}$, $L = 2\text{m}$	$\text{Sm}_2\text{Co}_{17}$ is employed (lower radiation damage)
2003	SPring-8	$\lambda_u = 15\text{mm}$, $G_{\min} = 2\text{mm}$, $L = 4.5\text{m}$	for SCSS project
2003	KEK	$\lambda_u = 40\text{mm}$, $G_{\min} = 10\text{mm}$, $L = 3.6\text{m}$	Tapered undulator
2003	SLS	$\lambda_u = 19\text{mm}$, $G_{\min} = 5\text{mm}$, $L = 1.9\text{m}$	Assembled at SPring-8
2004	ALS	$\lambda_u = 30\text{mm}$, $G_{\min} = 5\text{mm}$, $L = 1.5\text{m}$	Assembled at SPring-8
2006	SSRL	$\lambda_u = 22\text{mm}$, $G_{\min} = 5\text{mm}$, $L = 1.5\text{m}$	Assembled at SPring-8

Before the commissioning of the SPring-8 storage ring that started in March 1997, four IVUs were installed. Because the magnet gap (=vacuum gap) was fully opened at 50 mm, it had little effects on the storage ring operation. The first light from the IVU was measured on 23rd April 1997 at the beamline BL47XU. Commissioning of all the four IVUs was successfully completed by July 1997 [3], showing the feasibility of the IVUs as SR sources. To date, more than 20 IVUs, including exotic ones such as the in-vacuum helical undulator and 25-m long IVU, have been installed and operated in SPring-8 without serious problems.

Encouraged by the successful operation of IVUs at SPring-8, the SLS decided to adopt the IVU for the x-ray beamlines mainly dedicated to the protein crystallography [5]. In a first step, the IVU tested at ESRF has been modified and brought to SLS in 2000. As in SPring-8, it operated successfully and demonstrated to generate high-brilliance SR in the angstrom region. What should be noted is that high harmonics such as the 7th and 9th are utilized, meaning that the IVU has a good magnetic performance.

The utilization of IVU for high-brilliance x rays has now become a world trend. Especially in medium-scale SR facilities such as SLS, the IVU is regarded to be a promising way toward shorter wavelength.

KEY TECHNOLOGIES

In order to realize the IVU, a lot of technologies have to be developed. After the 1st IVU constructed in KEK, improvements have been made to various components in the IVU at the SPring-8, where more than 20 IVUs have

been installed. In the following sections, key technologies of the IVU are reviewed.

Overall Structure

Figure 1 shows an overall structure of the IVU. The magnet arrays are supported by two backing beams: in-vacuum and out-vacuum. The in-vacuum beam is usually made from aluminum and support the magnet arrays. The out-vacuum beam is connected to ball screws with girders to provide a gap movement. The ball screws are housed in a rigid support frame that limit deflections due to a magnetic attractive force, and actuated by driving motor(s). The two beams are connected by bellows shafts that shrink and expand according to the gap movement. Between the bellows shaft and out-vacuum beam, linear guides that allow a longitudinal movement of the bellows shaft are installed in order to compensate the thermal expansion at the time of bakeout.

Two types of components are installed for impedance reduction. One is the metal sheet that covers the magnet surface, and the other is the RF transition assembly to connect the magnet end and adjacent vacuum duct smoothly. After the beam test at ESRF, 50- μm copper sheet plated with 50- μm nickel has been used instead for the metal sheet.

Both the magnet arrays and RF transition assembly are equipped with cooling channels. In particular, the temperature of the cooling water for the magnet arrays is carefully controlled within $\pm 0.1^\circ\text{C}$, because the remanent field of PM material has a non-negligible temperature coefficient.

Although not shown in the figure, a lot of pumps are attached to the vacuum chamber. In the SPring-8 IVU, six ion

pumps with a pumping speed of 125l/sec and NEG pumps with 500l/sec are attached, resulting in a pumping speed of 6750l/sec in total.

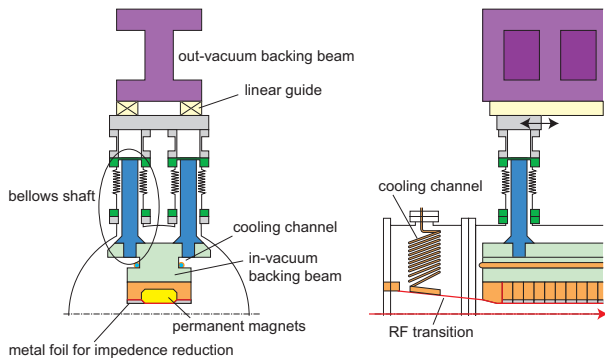


Figure 1: Schematic illustration of the IVU overall structure.

Permanent Magnet

Choice of PM material is one of the most important factors in the IVU design. Figure 2 shows characteristics of various PM materials in terms of remanent field and coercivity. In general, PMs with higher remanent field has lower coercivity. In IVUs, the PMs should be baked at a temperature at least higher than 100°C during the bakeout process to achieve UHV. In order to avoid irreversible demagnetization during bakeout, PMs with higher coercivity is required. In addition, PM material with higher coercivity is found to have a higher resistance to radiation damage[6]. From these points, PMs with coercivity higher than 2000 kA/m are employed in the IVUs.

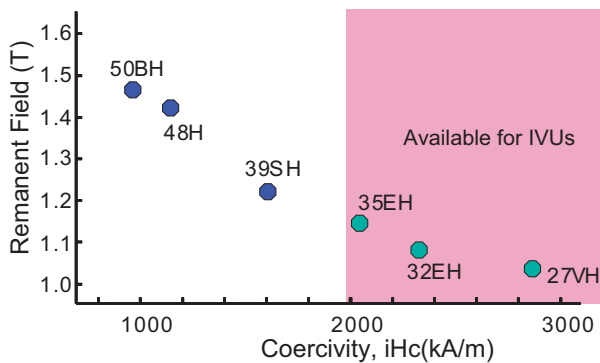


Figure 2: Various types of PM materials (NEOMAX**) and their characteristics. (Courtesy of NEOMAX Co., Ltd.)

TiN Coating

Because of a porous structure, the PM has significant outgassing when placed in vacuum, being an obstacle to realization of UHV. In the 1st IVU constructed in KEK, Ni

plating with a thickness of 25μm was used to suppress outgassing. However, it was not necessarily suited to installation in vacuum. In 1996, a technique of depositing TiN coating onto NdFeB magnets with a thickness of 5μm was developed and it was verified that the achievable vacuum was better than that of Ni plating [8]. Thus TiN coating has been employed as a standard technique for PM coating in the IVU. An example of the TiN-coated magnet sample is shown in Fig. 3.

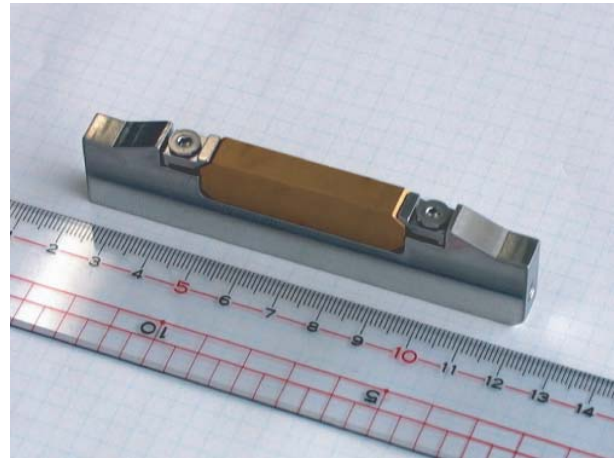


Figure 3: PM sample coated with TiN.

Field Correction

Because the PMs have unavoidable field error, the undulator field generated by them is far from ideal if no measures are taken. For example, the optical phase between adjacent periods fluctuates, resulting in degradation of brilliance, and multipole components of the integrated field cause unwanted effects on the storage ring operation. The undulator error field should be corrected so that these errors become negligible.

In conventional out-vacuum undulators, shimming, i.e., placing thin steel shims on the magnet surface, is used as a standard field-correction technique. In the IVU, however, the rough surface created by shimming induces wakefield, which may cause instability in the storage ring operation, when the electron beam passes through the IVU.

In SPring-8, an alternative method of field correction, called “in-situ sorting” has been developed [9]. It is based on rearrangement of PM blocks with an analysis of the entire undulator field mapping by scanning a Hall probe instead of individual measurement of each PM block. PM blocks are swapped and flipped to reduce the phase error and integrated multipole components. An example of the results of the in-situ sorting is shown in Fig. 4.

Impedance Reduction

After the field correction, two components to reduce the impedance, or the wakefield induced by interaction be-

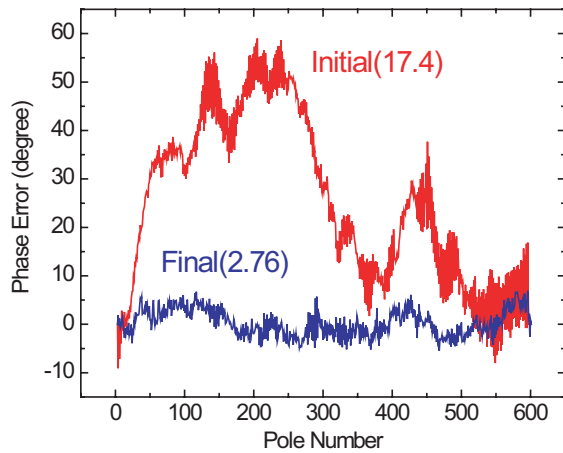


Figure 4: Example of the results of in-situ sorting. The r.m.s phase error is reduced from 17.4 to 2.76 degree.

tween the electron beam and components in the IVU, are installed. They are explained in the following sections.

Magnet Cover The electric conductivity of TiN and NdFeB is not very good. Moreover, there is an interval (several tens of microns) between adjacent PM blocks, i.e., discontinuity exists. In order to avoid wakefield induced by these factors, the PM array is covered with a metal sheet. After the beam test at ESRF, a $50\mu\text{m}$ -thick Cu sheet coated with $50\mu\text{m}$ -thick Ni is used as a standard magnet cover. From the power spectrum of the resistive wall heating [10] calculated for the bunch profile of the electron beam in SPring-8, it has been verified that $50\mu\text{m}$ is thick enough to be regarded as infinite in terms of the power production in the sheet. The thickness of the Ni sheet has been determined so that it generates attractive force enough for a rigid contact between the sheet and PM blocks. Photograph of the magnet array covered with the Cu sheet is shown in Fig. 5.

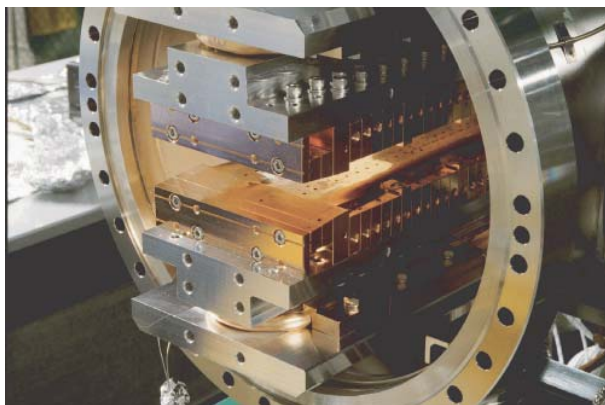


Figure 5: Magnet array covered with Cu sheet for impedance reduction.

RF Transition The RF transition assembly, shown in Fig. 6, plays a role to smoothly connect the magnet end and adjacent vacuum duct. It should also follow the gap movement of the magnet arrays. In general, it is made from Cu and is equipped with cooling channels to remove the heat brought by the electron beam during operation.

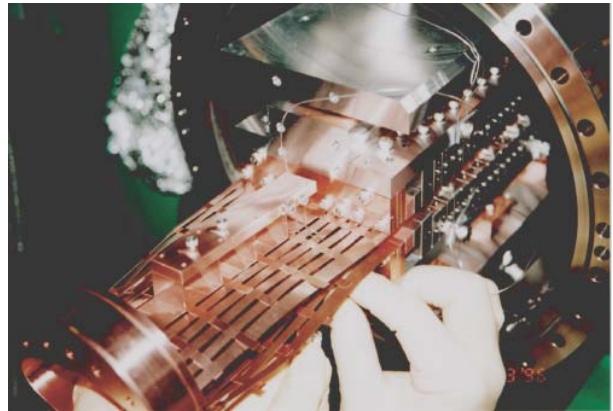


Figure 6: RF transition assembly to smoothly connect the magnet end and adjacent vacuum duct.

UHV Bakeout

After assembling all the components, the IVU system should be baked to reach UHV levels for installation in the storage ring. The temperature for the bakeout is about 200°C for the vacuum chamber and 125°C for the magnet arrays. The PM blocks are pre-baked at a temperature slightly higher than that at the bakeout, e.g., 140°C , which effectively reduces the demagnetization during bakeout. In addition, this procedure improves the resistance to radiation of PMs [7].

During heating up to the above temperature, relative position between the vacuum chamber and the bellows shaft, or the in-vacuum beam, should be monitored. The temperature of the vacuum chamber made from SUS and in-vacuum beam made from Al should be controlled so that difference in the thermal expansion between SUS and Al does not break either the bellows shaft or the RF transition assembly.

EXOTIC IN-VACUUM UNDULATORS AT SPRING-8

Besides the standard IVU with $\lambda_u=32\text{mm}$ and $L=4.5\text{m}$, a number of exotic IVUs have been developed at SPring-8. Explanations of them are given in the following sections.

Figure-8 Undulator

The figure-8 undulator is an ID proposed at SPring-8 to provide linearly polarized radiation in the soft x-ray region [12]. The electron trajectory looks a figure of eight when projected onto the transverse plane. The most important

advantage is that most of the radiation power brought by high harmonics diverges off axis, resulting in a low heat load on optical elements as well as the helical undulator. In addition, both the horizontal and vertical polarizations are obtained simultaneously. An in-vacuum figure-8 undulator for a hard x-ray region was constructed in 1997 [13] and installed in BL24XU in SPring-8, where experiments that takes advantage of the polarization characteristics of the figure-8 undulator are carried out. An example of spectrum is shown in Fig. 7.

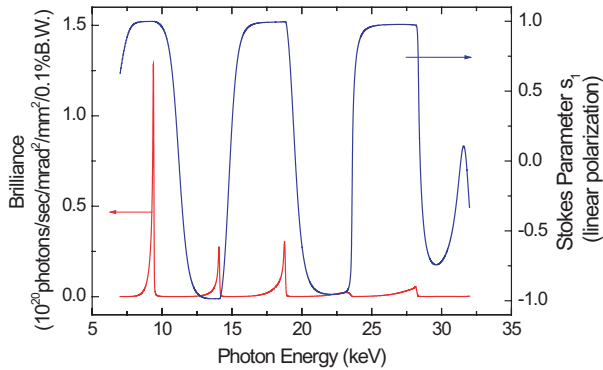


Figure 7: Spectrum of brilliance and stokes parameter s_0 that denotes the fraction of horizontal and vertical polarization components obtained for the in-vacuum figure-8 undulator.

Helical Undulator

The in-vacuum helical undulator [11] was constructed in 1999 and installed in BL40XU in SPring-8. The magnet array, shown in Fig. 8, has a complicated configuration in order to improve the field uniformity and keep the helical-undulator condition ($B_x \sim B_y$) for a wide gap range. It should be noted that the helicity of circular polarization cannot be changed. The main purpose of this undulator is to provide high-flux fundamental radiation with little high harmonics. The quasimonochromatic x-ray is focused with focusing mirrors and is applied directly to samples without a monochromator. For example, a photon flux of 1.5×10^{15} is obtained with a bandwidth of 1.5% at a photon energy of 10keV.

Revolver Undulator

The concept of a revolver undulator is to mount a number of magnet arrays with different period lengths on a rotary beam so that an adequate one can be selected according to the radiation wavelength required for experiments. An in-vacuum undulator of this type was constructed in 2000 [14]. In this device, four magnet arrays with periodic lengths of 6, 10, 15, and 20 mm were installed as shown in Fig. 9. In order to compensate the magnetic attractive force, additional magnet arrays that generate a repulsive force are mounted on the both side of the rotary

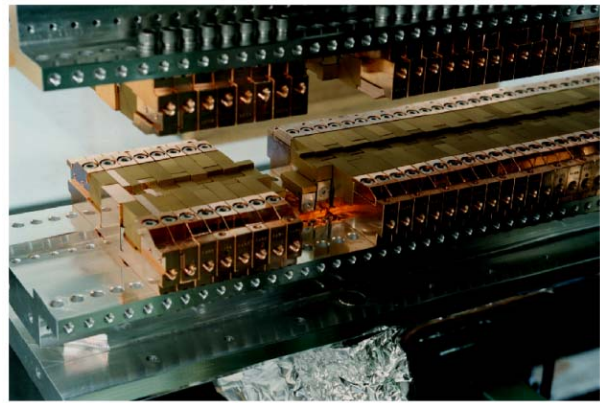


Figure 8: Magnet array of the in-vacuum helical undulator.

beam, which makes it possible to support the beam just at both ends. Thanks to this, the rotary beam can be rotated by 360° . In 2003, the magnet array with the period length of 6mm has been replaced by that with 24mm and brought to Pohang Light Source in Korea to provide high-brilliance SR in the x-ray region.

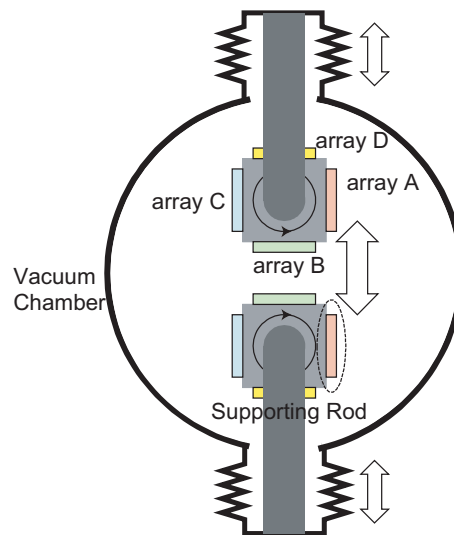


Figure 9: Schematic illustration of the in-vacuum revolver undulator.

25-m Undulator

SPring-8 storage ring has four 30-m long straight sections (LSSs). A 25-m long IVU was constructed and installed in one of the LSSs in 2000 [15] as shown in Fig. 10. It is composed of five segments with a length of 5m. Each segment was assembled outside the storage ring and transported individually. After transporting all the segments, they were connected with each other.

Field measurement and correction have been carried out as follows [16]. Firstly, normal field measurement and correction were made for each segment. Secondly, the magnetic field in junctions between segments was measured.

Then, the gap discrepancy between segments, which gives rise to a large phase error, was corrected. Finally, the whole magnetic distribution has been obtained by combination of the fields in five segments and in four junctions.



Figure 10: 25-m long IVU installed in the LSS in SPring-8.

After installation in the LSS, effects on the electron beam were investigated with the gap closed down to 12 mm, and no serious problems were found except a slight degradation of the beam lifetime. After that the radiation spectrum was measured to estimate the performance of the 25-m IVU as a SR light source and it was found that the bandwidth was a little wider than expected. After investigation of several factors, it was concluded that the geomagnetic field would be the most probable source, because the direction of the undulator, in which the field corrections were carried out, differed by 90° from the direction of installation in the storage ring. In order to correct it, a uniform field was applied to cancel the geomagnetic field. As a result, the bandwidth was reduced to ideal one [17]. This fact shows that the field measurement and correction carried out for the 25-m IVU were very precise.

ADVANTAGES IN THE X-RAY FEL

IVUs installed in the storage ring have been described so far. As a matter of course, the IVU can be utilized as a driver for the FEL. In fact, the SCSS [18] and PALXFEL [19] projects are going to adopt the IVU with periodic length shorter than 20 mm to realize an x-ray FEL with less electron energy, smaller facility scale, and thus lower cost.

Besides the advantage of reducing the electron energy, the IVU has several advantages over the conventional out-vacuum undulator when employed in the X-ray FEL facility where a very long undulator is required for saturation.

Alignment using Optical Laser

An alignment procedure using an optical laser beam is proposed for the SCSS project in order to align the BPMs installed in the undulator line [20]. The diffraction pattern

of the laser beam generated by an iris inserted in the BPM positions is monitored with a CCD camera installed downstream. For this to be applicable, it is necessary to let the optical laser pass through the entire undulator line, meaning that a wide clearance for the optical path is required. It is easy for the IVU to realize it because the vacuum gap is variable unlike the out-vacuum undulators.

Commissioning

The variable vacuum gap is also useful for the initial commissioning of the electron beam. The wide clearance created by fully opening the gap will make it easier. In addition, it is also important for the “FEL commissioning”, or the on-beam alignment of components installed in the undulator line such as the BPMs, undulators, phase shifters, and correction coils. It is to be carried out by monitoring the spontaneous radiation emitted from one or two adjacent undulator segments. If the vacuum gap is narrow, then the spontaneous radiation emitted near the entrance of the undulator line may be disturbed by the undulator segment near the exit.

R&DS UNDER PROGRESS

In SPring-8, a number of R&Ds are under progress for future improvement of the IVU and related technology. Two of them are introduced in the following sections.

Cryoundulator

As mentioned in the “Permanent Magnet” section, PMs with high coercivity should be chosen for the IVU to avoid irreversible demagnetization during the bakeout process and due to radiation damage, which in turn limits the achievable peak field because such PMs have relatively low remanent field. For example, the remanent field and coercivity of NEOMAX35EH, which is the PM material normally used for the IVU, are 1.15T and 2000kA/m, respectively.

Now let us assume that the magnet arrays are cooled down to be operated at a cryogenic temperature. Then, outgassing from the PM blocks are reduced considerably; rather, the magnet array may work as a cryopump, meaning that the bakeout process is no more necessary. In addition, the PM characteristics are improved a lot because both the remanent field and coercivity normally have a negative temperature coefficient. For example, the remanent field and coercivity of NEOMAX50BH at a temperature of 140K, which has the highest remanent field among the PM materials that are commercially available, are found to be 1.58T and 3000kA/m, respectively. Compared these values to those of NEOMAX35EH, we can expect a 40% increase in peak field and a higher resistance to radiation damage. This is the concept of the cryogenic permanent magnet undulator, or the cryoundulator [21].

From the experiments to investigate the temperature dependence of PM material, it has been found that the rema-

ment field has its maximum at a temperature around 140K, which is the optimum operating temperature of the cryo-undulator. This means that the cryo-undulator can be realized by a slight modification of the IVU, because the magnet arrays of the IVU are placed in vacuum and thus is thermally insulated. The state-of-the-art cryocooler has a cooling capacity of 200W at a temperature around 80K, meaning that the heat load brought by the electron beam and SR from the upstream bending magnet may not be a serious problem. This is contrary to superconducting undulators operated at a temperature around the liquid helium [22].

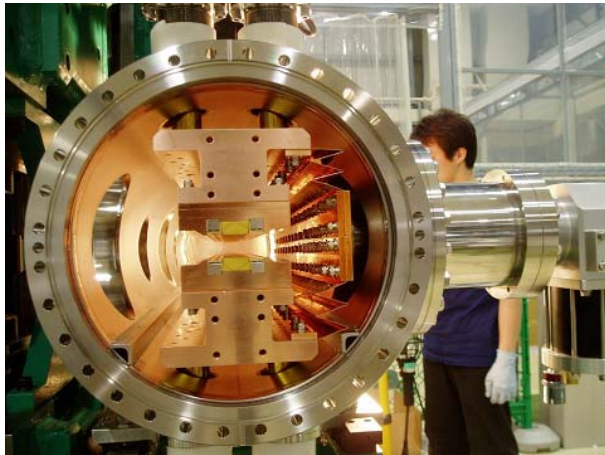


Figure 11: Cryo-undulator prototype under development in SPring-8.

In SPring-8, a prototype of the cryo-undulator is now under development as shown in Fig. 11. NEOMAX50BH has been employed as PM material, and the period length and number of periods are 15mm and 40, respectively. Figure 12 shows a preliminary result of field measurement. As expected, the peak field is enhanced as the operating temperature is reduced.

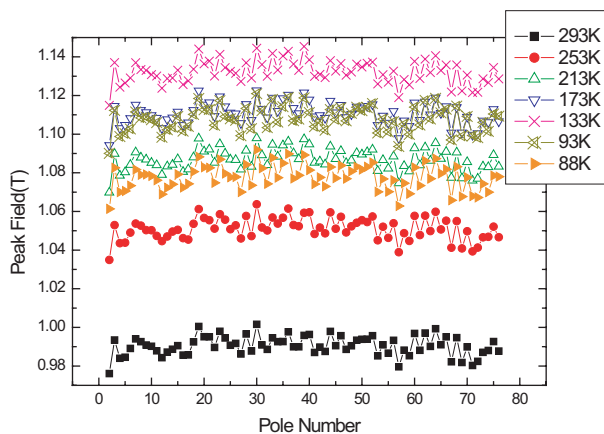


Figure 12: Results of the field measurement for the cryo-undulator prototype. The peak field is plotted as a function of the pole number for various operating temperatures.

In-situ Field Measurement

In order to assemble the vacuum chamber, the magnet arrays should be taken off after the field correction is finished. It is therefore necessary to ensure that the magnetic field is unchanged meanwhile. The most straightforward way is to measure the magnetic field after assembly, which is not very easy because the vacuum chamber itself becomes an obstacle for Hall-probe scanning. Instead, we rely on the accuracy of assembling the components, especially, the bellows shaft. We control the torque for connecting the bellows shafts with the in-vacuum and out-vacuum beams. During construction of the 1st IVU for SPring-8, we just detached and attached the magnet arrays without installing the vacuum chamber and compared the magnetic field in order to check the accuracy of assembly, and found no significant difference. It should be noted, however, that the magnetic field is more sensitive to the gap value for shorter wavelength, meaning that the accuracy of assembly may be more stringent. In addition, especially utilized as an FEL driver, the magnetic field change, due to radiation damage and aging effects of the support frame and PM material, may have to be monitored for a long period. This requires a portable field-measurement system that enables a measurement without taking off the vacuum system. Let us call it an “in-situ field measurement” system.

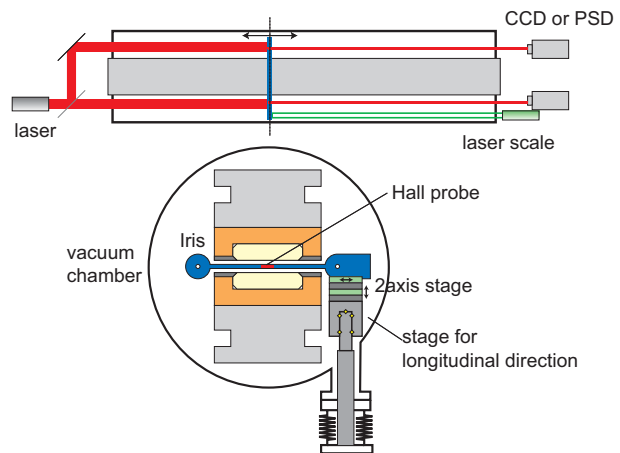


Figure 13: Schematic illustration of the in-situ field measurement system under proposal.

Figure 13 shows a schematic illustration of the in-situ field measurement under proposal. The z-axis stage scans the Hall probe as the conventional field measurement system. What is important is that the actuation errors of the z stage, such as the pitching and rolling, do not have to be necessarily low. Although these errors cause a fluctuation of the transverse position of the Hall probe, they are detected with the photo detector located downstream by measuring the central position of the diffraction pattern created by the iris attached to the Hall probe module. This is an application of the BPM alignment procedure proposed at the SCSS project [18]. The Hall probe position can be kept on the undulator axis by calling a feedback loop. The

longitudinal position is detected by a laser scale that has a sub-micron resolution.

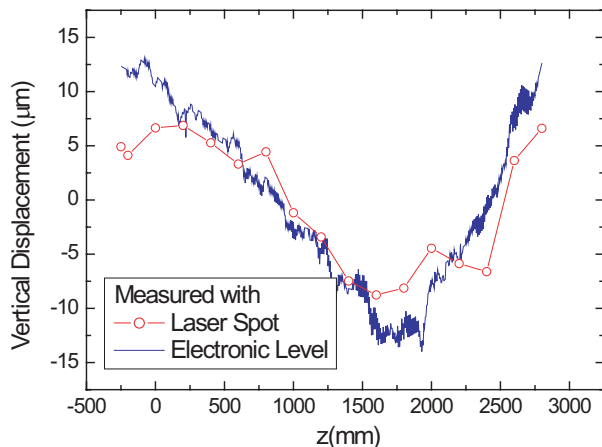


Figure 14: Vertical fluctuation of the granite field-measurement bench measured with the laser spot and electronic level.

What is the most important in the above system is the measurement of the transverse Hall probe position. In order to demonstrate it, we have measure the vertical displacement of the field-measurement bench made from granite usually used for the Hall probe scanning. The results are shown in Fig. 14 together with the results of a measurement using electronic levels. We can find that they are in good agreement. In this measurement, we used a CCD camera to measure the laser spot profile and transferred it to a PC to take an average and calculate the center of the gravity, which takes about 10 seconds per measurement. We have recently tested a PSD (position sensitive detector) for higher measurement speed. As a result, the measurement time was improved by two orders of magnitude with the spatial resolution better than or equal to the CCD.

SUMMARY

The IVU is now an ordinary (=reliable), but not a special (=risky) means for shorter wavelength with higher brilliance and provides a possibility of hard x-ray experiments in a medium-scale SR facilities. In addition, the variable “vacuum gap” is very useful in various ways as follows. Firstly, the IVUs can be installed before starting the commissioning of the storage ring as in SPring-8, which is not the case for the out-vacuum undulators because it inevitably creates a narrow aperture in the ring. Secondly, the wide clearance is useful for the initial commissioning and alignment using optical laser for the SASE FEL facility.

Although not described in this paper, R&Ds to apply high-temperature superconductors (HTSCs) to SR sources are in progress [23]-[24]. This scheme requires a zero gap to magnetize the HTSCs, which is realized only by the IVU.

REFERENCES

- [1] S. Yamamoto, T. Shioya, M. Hara, H. Kitamura, X. W. Zhang, T. Mochizuki, H. Sugiyama and M. Ando, *Rev. Sci. Instrum.* 63 (1991) 400
- [2] T. Hara, T. Tanaka, T. Tanabe, X. Marechal, S. Okada and H. Kitamura, *J. Synchrotron Rad.* 5 (1998) 403
- [3] H. Kitamura, *J. Synchrotron Rad.* 5 (1998) 184
- [4] T. Hara, T. Tanaka, T. Tanabe, X. Marechal, H. Kitamura, P. Elleaume, B. Morrison, J. Chavanne, P. Vaerenbergh and D. Schmidt, *J. Synchrotron Rad.* 5 (1997) 406
- [5] T. Schmidt, G. Ingold, A. Imhof, B. Patterson, L. Patthey, C. Quitmann, C. Schulze-Briese, R. Abela, *Nucl. Instrum. Meth.* A467-468 (2001) 126
- [6] T. Bizen, Y. Asano, T. Hara, X. Marechal, T. Seike, T. Tanaka, H. Kitamura, H. S. Lee, D. E. Kim, C. W. Chung, *Proc. SRI2003*, 167
- [7] T. Bizen, Y. Asano, T. Hara, X. Marechal, T. Seike, T. Tanaka, H. Kitamura, H. S. Lee, D. E. Kim, C. W. Chung, *Proc. SRI2003*, 171
- [8] M. Ikegami, F. Kikui, S. Okada and T. Kohda, Sumitomo Special Metals Co., Ltd. internal report (in Japanese)
- [9] T. Tanaka, T. Seike, and H. Kitamura, *Nucl. Instrum. Meth.* A465 (2001) 600
- [10] K. Bane and S. Krinsky *Proc. PAC1993*, 3375
- [11] T. Hara, T. Tanaka, T. Seike, T. Bizen, X. Marechal, T. Kohda, K. Inoue, T. Oka, T. Suzuki, N. Yagi and H. Kitamura, *Nucl. Instrum. Meth.* A467-468 (2001) 165
- [12] T. Tanaka and H. Kitamura, *Nucl. Instrum. Meth.* A364 (1995) 368
- [13] T. Tanaka, X. Marechal, T. Hara, T. Tanabe and H. Kitamura, *J. Synchrotron Rad.* 5 (1998) 412
- [14] T. Bizen, T. Hara, X. Marechal, T. Seike, T. Tanaka and H. Kitamura, *Proc. SRI2003* 175
- [15] H. Kitamura, T. Bizen, T. Hara, X. Marechal, T. Seike and T. Tanaka, *Nucl. Instrum. Meth.* A467-468 (2001) 110
- [16] T. Tanaka, T. Seike, X. Marechal, T. Bizen, T. Hara and H. Kitamura, *Nucl. Instrum. Meth.* A467-468 (2001) 149
- [17] T. Hara, M. Yabashi, T. Tanaka, T. Bizen, S. Goto, X. Marechal, T. Seike, K. Tamasaku, T. Ishikawa and H. Kitamura, *Rev. Sci. Instrum.* 73 (2002) 1125
- [18] T. Tanaka, these proceedings, see also <http://www-xfel.spring8.or.jp/>
- [19] I. S. Ko, these proceedings.
- [20] T. Shintake, *Proc. APAC2004*
- [21] T. Hara, T. Tanaka, H. Kitamura, T. Bizen, T. Seike, T. Kohda, and Y. Matsuura, *Phys. Rev. ST-AB* 7 (2004) 050702.
- [22] R. Rossmanith, H. Moser, A. Geisler, A. Hohl, D. Krischel, and M. Schillo, *Proc. EPAC2002* 2628.
- [23] T. Tanaka, T. Hara, H. Kitamura, R. Tsuru, T. Bizen, X. Marechal and T. Seike, *Phys. Rev. ST-AB* 7 (2004) 090704.
- [24] T. Tanaka, R. Tsuru and H. Kitamura, *J. Synchrotron Rad.* 12 (2005) 442